Cell Reports, Volume *28*

Supplemental Information

A Hyperactive Form of *unc-13* Enhances Ca^{2+} Sensitivity and Synaptic Vesicle Release Probability in *C. elegans*

Lei Li, Haowen Liu, Qi Hall, Wei Wang, Yi Yu, Joshua M. Kaplan, and Zhitao Hu

Figure S1

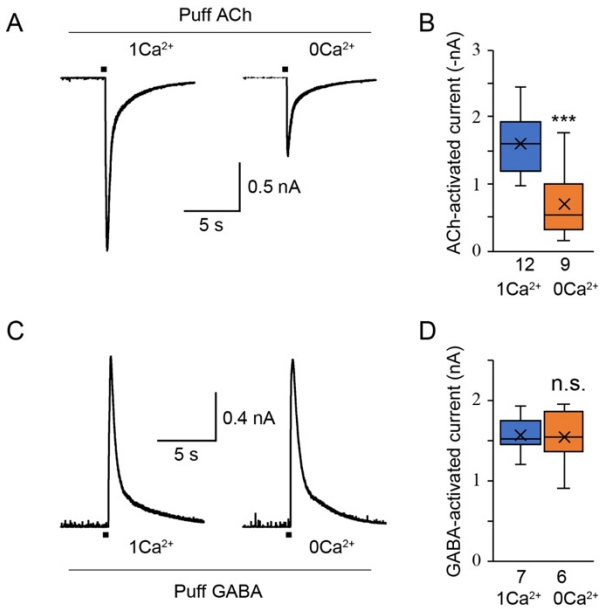

Figure S1. The channel conductance of ACh receptors is reduced in 0mM Ca^{2+}. Related to Figure 1. (A) Example traces of ACh-activated currents recorded from wild-type animals in 1mM and 0mM Ca^{2+} bath solutions. (B) Boxplot of the currents from A. (C) Example traces of GABA-activated currents recorded in 1mM and 0mM Ca^{2+} bath solutions, respectively. (D) Boxplot of the amplitude of the currents from C. Data are presented as box-and-whisker plots with the median (line) and mean (cross) indicated (***, $p < 0.001$ when compared to the 1mM Ca^{2+} recordings; n.s., non-significant when compared to the 1mM Ca^{2+} recordings; student's t-test). The number of worms analyzed for each genotype is indicated under each box.

Figure S2

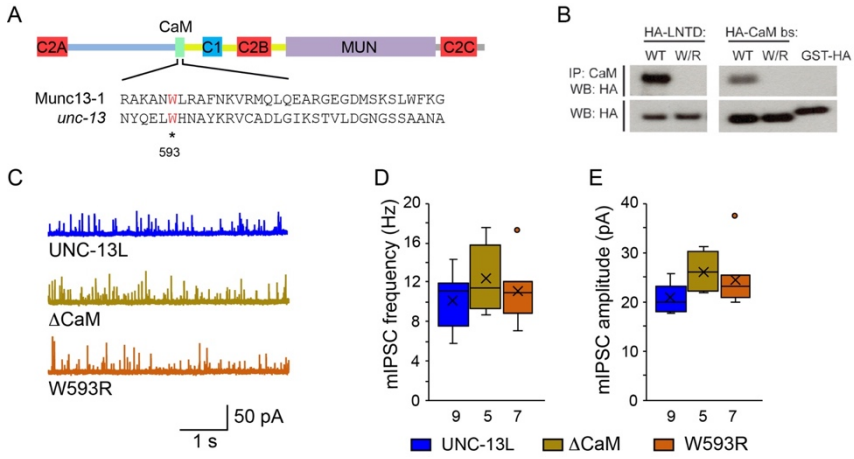

Figure S2. Effects of calmodulin binding UNC-13L on tonic release. Related to Figure 1. (A) Sequence alignment of the CaM domain between worm *unc-13* and rat Munc13-1. (B) Co-immunoprecipitation shows binding of the UNC-13L CaM domain and calmodulin. The binding is disrupted by mutating the conserved tryptophan (W593) to arginine (R) in the CaM domain. (C-E) Example traces of the mIPSCs and averaged mIPSC frequency and amplitude from the indicated genotypes. Data are presented as box-and-whisker plots with the median (line) and mean (cross) indicated (n.s., non-significant when compared to the UNC-13L rescue; D, one-way ANOVA; E, one-way ANOVA following Dunn's test). The number of worms analyzed for each genotype is indicated under each box.

Figure S3

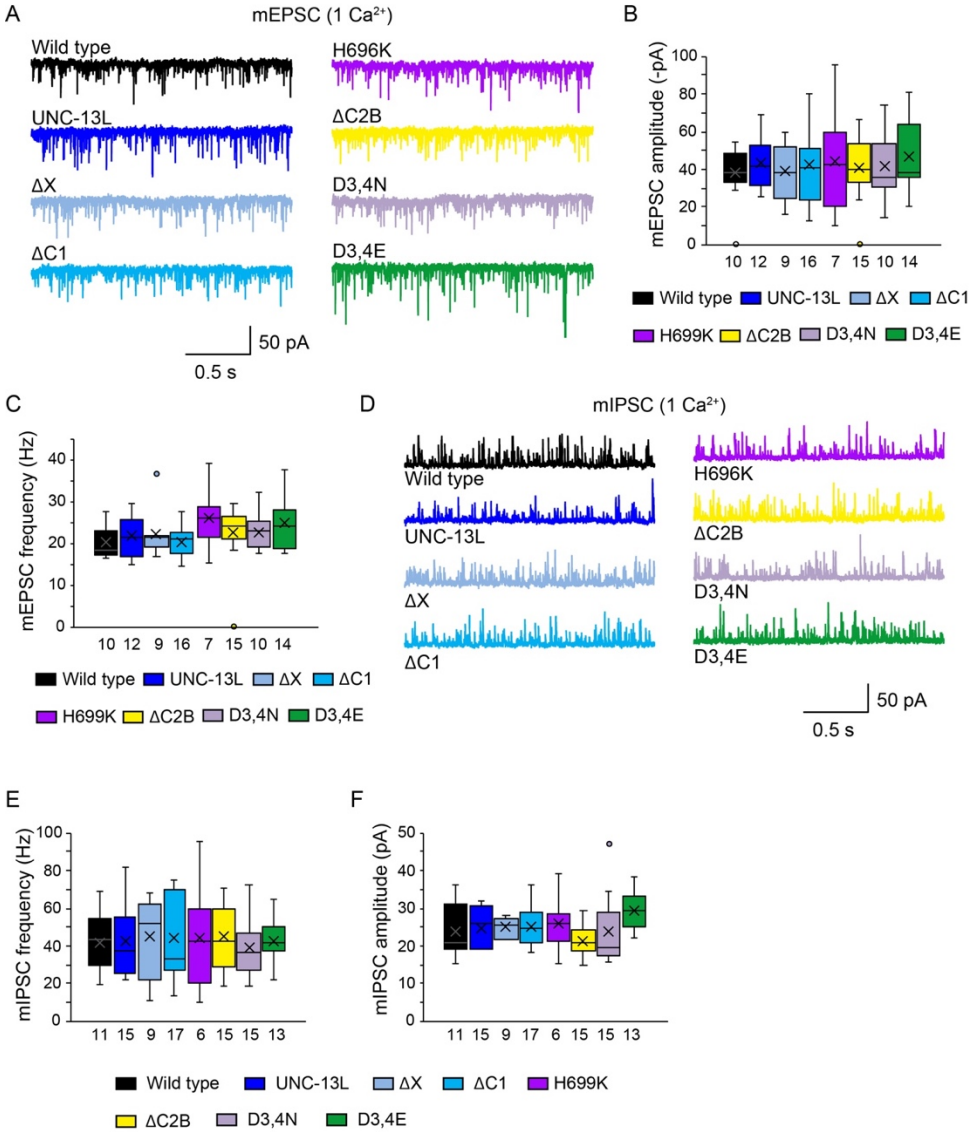

Figure S3. Tonic release in 1mM Ca^{2+} is unaltered by disrupting single domain function in UNC-13L. Related to Figure 2. (A) Representative mEPSC traces recorded from *unc-13* mutants rescued by the indicated constructs in 1mM Ca^{2+}. (B, C) Boxplot of mEPSC frequency and amplitude from the indicated genotypes in A. (D) Representative mIPSC traces recorded from *unc-13* mutants rescued by the indicated constructs in 1mM Ca^{2+}. (E, F) Boxplot of mIPSC frequency and amplitude from the indicated genotypes in D. Data are shown as box-and-whisker plots with the median (line) and mean (cross) indicated (one-way ANOVA for data in B, E, one-way ANOVA following Kruskal-Wallis test for data in C, F). The number of worms analyzed for each genotype is indicated under each box.

Figure S4

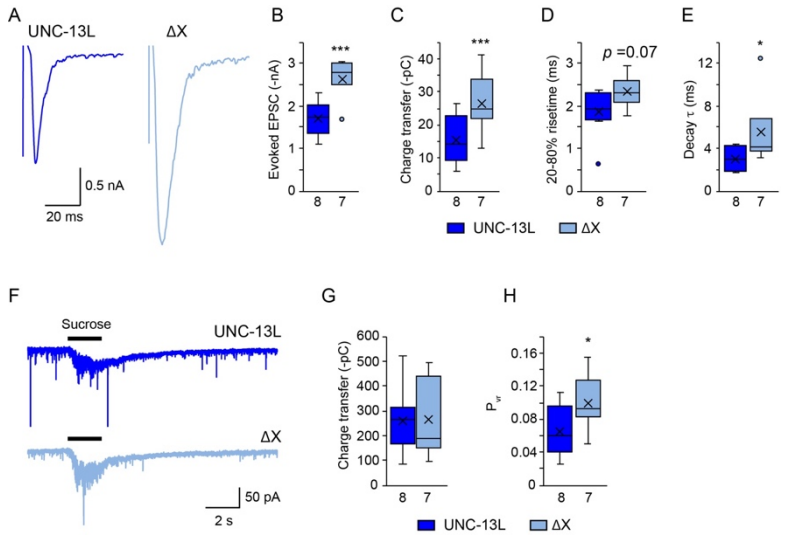

Figure S4. The X domain inhibits evoked neurotransmitter release but not priming. Related to Figure 3. (A) Example traces of stimulus-evoked EPSCs recorded in 1mM Ca^{2+} from UNC-13L rescue (blue) and UNC-13LΔX rescue (red) animals. (B-E) Quantification of the evoked EPSC amplitude, charge transfer, 20-80% risetime, and decay from the same genotypes as in A. (F) Hypertonic sucrose-evoked current recorded from UNC-13L rescue (blue) and UNC-13LΔX rescue (red) animals. (K) Averaged charge transfer from the sucrose-evoked currents in F. (L) Quantification of the probability of synaptic vesicle release (P_{vr}) from the indicated genotypes. Data are shown as box-and-whisker plots with the both median (line) and mean (cross) indicated (*, $p < 0.05$, ***, $p < 0.001$ when compared to the UNC-13L rescue; Mann-Whitney test for data in E, student's t-test for all others). The number of worms analyzed for each genotype is indicated under each box.

Figure S5

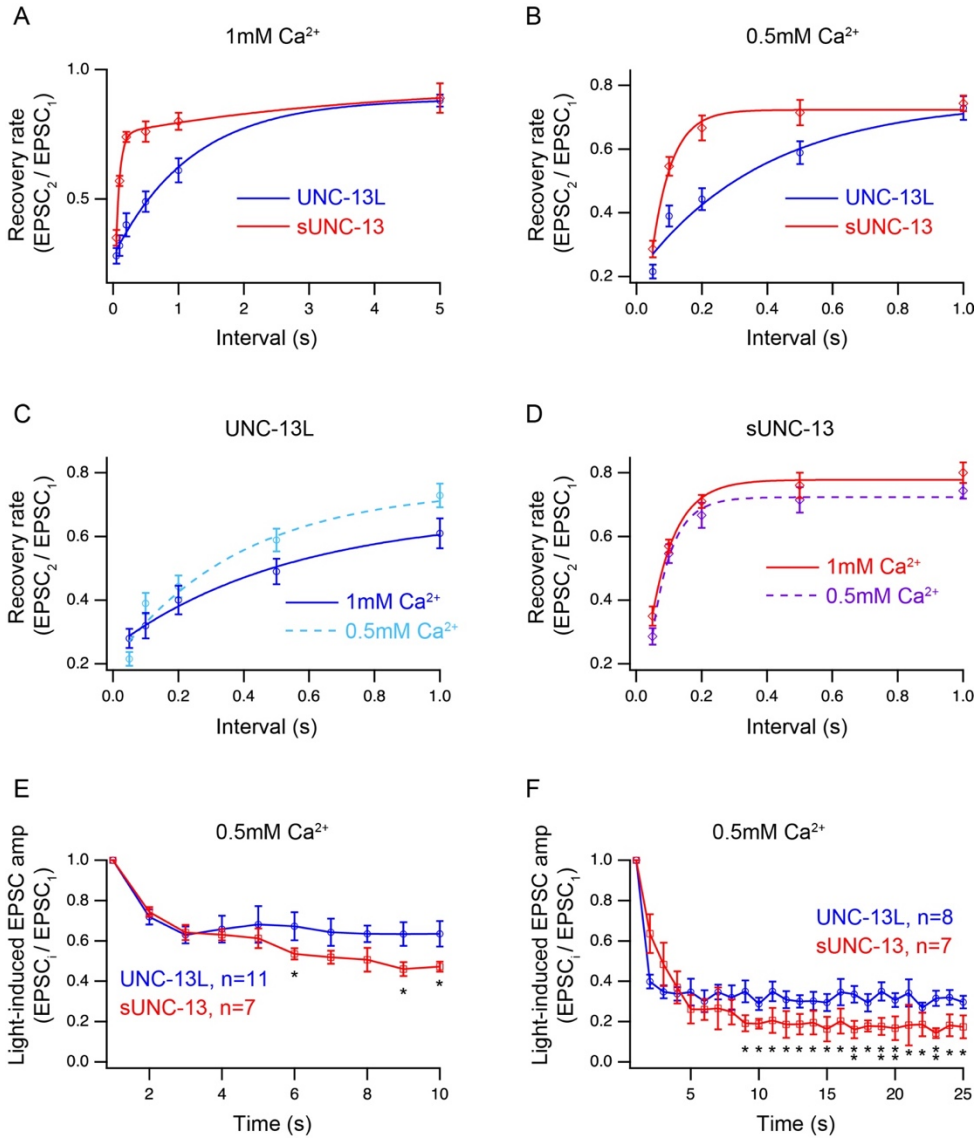

Figure S5. Synaptic recovery and depression in 0.5mM Ca^{2+}. Related to Figure 4. Averaged synaptic recovery rescued by UNC-13L and sUNC-13 in 1mM Ca^{2+} (A) and 0.5mM Ca^{2+} (B). The recovery rate was calculated by the ratio of $EPSC_2$ to $EPSC_1$ in the paired stimulus. (C, D) Comparison of synaptic recovery between 1mM and 0.5mM Ca^{2+} in the same genotype. (E, F) Quantification of synaptic depression by normalizing the EPSC amplitude ($EPSC_i$) to the first EPSC amplitude in 0.5mM Ca^{2+}. Data are mean ± SEM ((*, $p < 0.05$, **, $p < 0.01$ when compared to the UNC-13L rescue; student's t-test).

Figure S6

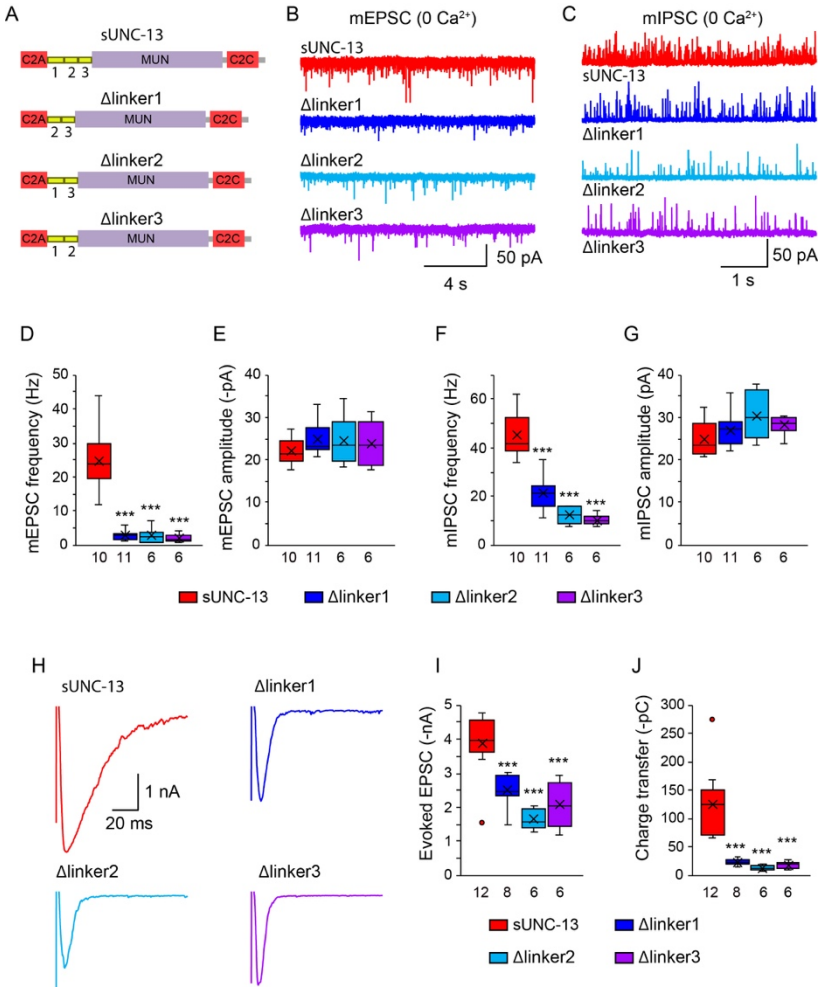

Figure S6. The three small linkers are essential for sUNC-13 function. Related to Figure 5. (A) Cartoon depicting the domain structure of sUNC-13, Δlinker1, Δlinker2, and Δlinker3. (B-G) Representative traces and boxplot of frequency and amplitude of mEPSCs and mIPSCs recorded from the indicated genotypes in 0mM Ca^{2+}. (H-J) Representative traces and summary of the amplitude and charge transfer of the evoked EPSCs recorded from the indicated genotypes in 1mM Ca^{2+}. Data are shown as box-and-whisker plots with the both median (line) and mean (cross) indicated (***, $p < 0.001$ when compared to the sUNC-13 rescue; one-way ANOVA test for data in E, F, G, one-way ANOVA following Kruskal-Wallis test for data in D, I, J). The number of worms analyzed for each genotype is indicated under each box.

Figure S7

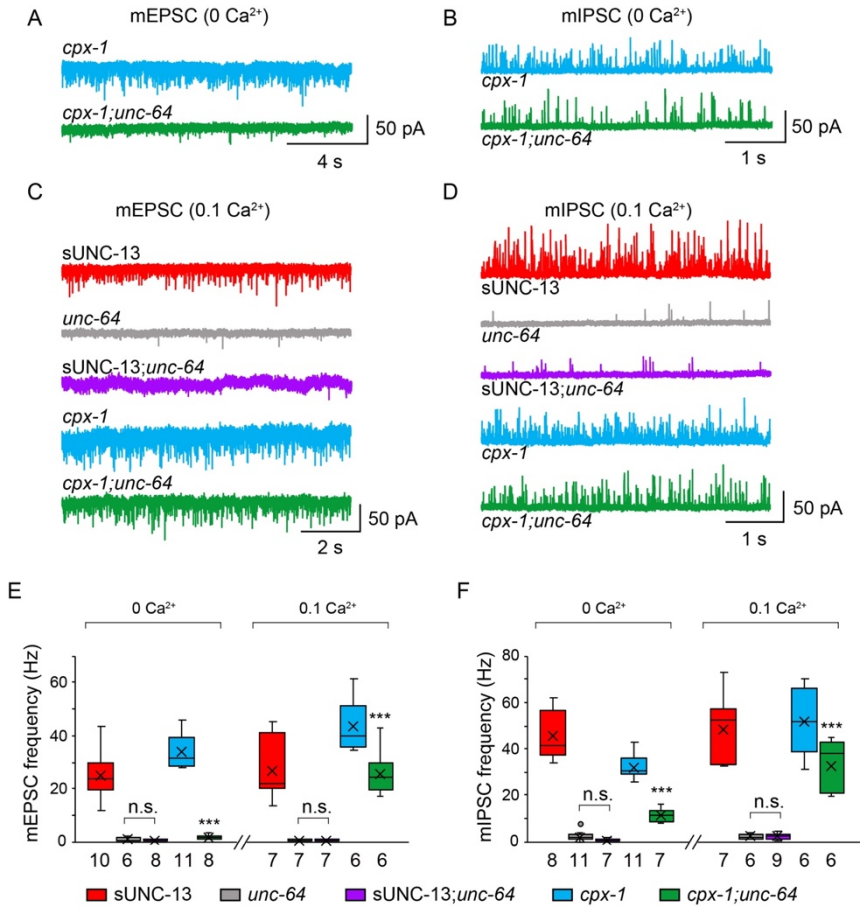

Figure S7. Tonic release in sUNC-13 rescue but not in *cpx-1* mutants is blocked when *unc-64*/syntaxin-1A is lacking. Related to Figure 7. (A-D) Representative traces of the mEPSCs and mIPSCs recorded from the indicated genotypes in 0mM and 0.1mM Ca^{2+}. (E, F) Averaged frequencies of the mEPSC and mIPSC from the indicated genotypes. Data are shown as box-and-whisker plots with the both median (line) and mean (cross) indicated (***, $p < 0.001$ when compared to sUNC-13;*unc-64*; n.s., non-significant; one-way ANOVA). The number of worms analyzed for each genotype is indicated under each box.

Table S1. Summary of the electrophysiological data in this study. Related to Figure 1-7.

	Tonic release								evoked EPSC		RRP	P_{vr}
	mEPSC (0mM Ca^{2+})		mEPSC (1mM Ca^{2+})		mIPSC (0mM Ca^{2+})		mIPSC (1mM Ca^{2+})					
	Frequency (Hz)	Amplitude (-pA)	Frequency (Hz)	Amplitude (-pA)	mIPSC (Hz)	Amplitude (pA)	mIPSC (Hz)	Amplitude (pA)	Amplitude (-nA)	Charge (-pC)	Charge (-pC)	
Wild type	1.9 ± 0.2	23.2 ± 1.6	43.5 ± 4.3	23.9 ± 1.1	10.9 ± 1.1	25.9 ± 1.1	42.5 ± 4.1	22.5 ± 2.1	2.3 ± 0.2	20.6 ± 2.1	221 ± 23.1	0.09 ± 0.01
unc-13(s69)	0.1 ± 0.01	20.2 ± 3	0.5 ± 0.09	21.1 ± 2.1	0.1 ± 0.01	22.1 ± 4.1	0.6 ± 0.02	21.5 ± 3.2	0.01 ± 0.01	0.05 ± 0.01	25.5 ± 7.1	0
UNC-13L	1.5 ± 0.4	19.3 ± 1.9	43.4 ± 3.7	23.9 ± 1.1	10.1 ± 0.9	22.3 ± 2.2	38.1 ± 3.5	22.4 ± 1.1	1.7 ± 0.1	15.4 ± 2.6	237 ± 25.4	0.06 ± 0.01
UNC-13LΔX	1.1 ± 0.2	22.8 ± 0.9	39.1 ± 5.0	22.2 ± 1.9	14.3 ± 0.5	24.8 ± 1.5	44.9 ± 8.9	24.9 ± 1.1	2.6 ± 0.2	26.6 ± 2.9	266 ± 47.4	0.1 ± 0.01
UNC-13LΔC1	2.2 ± 0.7	19.3 ± 1.9	42.3 ± 4.9	20.3 ± 0.8	18.8 ± 2.7	24.7 ± 0.9	43.9 ± 5.4	25.2 ± 1.3	2.1 ± 0.2	20.4 ± 2.6	Ref. Michelassi et al.	Ref. Michelassi et al.
UNC-13LΔC2B	2.8 ± 0.3	20.9 ± 2.5	43.4 ± 3.3	24.4 ± 0.8	25.8 ± 2.6	25.7 ± 1.7	53.2 ± 4.2	25.2 ± 1.3	2.7 ± 0.1	26.5 ± 1.9	Ref. Michelassi et al.	Ref. Michelassi et al.
UNC-13L(H696K)	1.7 ± 0.3	19.7 ± 3.0	36.3 ± 3.4	20.8 ± 1.8	16.9 ± 1.2	25.2 ± 1.0	44.3 ± 10.6	26.0 ± 2.7	1.6 ± 0.2	14.7 ± 2.9	n/a	n/a
UNC-13L(D3,4N)	2.6 ± 0.6	24.8 ± 1.9	41.6 ± 4.2	22.7 ± 1.1	24.7 ± 4.6	23.4 ± 0.4	39.1 ± 5.2	20.9 ± 1.9	2.8 ± 0.1	31.3 ± 4.4	n/a	n/a
UNC-13L(D3,4E)	0.7 ± 0.06	20.2 ± 1.5	46.9 ± 5.0	24.7 ± 1.6	7.7 ± 0.9	25.9 ± 2.0	42.8 ± 3.4	31.1 ± 2.8	1.6 ± 0.2	8.3 ± 1.3	n/a	n/a
UNC-13L(D1-5N)	4.4 ± 0.5	25.2 ± 2.2	n/a	n/a	32.9 ± 1.3	27.5 ± 0.7	n/a	n/a	n/a	n/a	n/a	n/a
UNC-13LΔCaM	1.3 ± 0.3	20.1 ± 3.1	n/a	n/a	12.3 ± 1.6	27.5 ± 2.1	n/a	n/a	n/a	n/a	n/a	n/a
UNC-13L(W593R)	1.2 ± 0.4	19.1 ± 2.5	n/a	n/a	10.9 ± 1.7	26.5 ± 3.8	n/a	n/a	n/a	n/a	n/a	n/a
sUNC-13	24.7 ± 2.8	22.1 ± 0.9	41.1 ± 2.2	23.5 ± 0.9	45.3 ± 3.0	24.9 ± 1.4	45.3 ± 3.8	23.3 ± 1.0	3.9 ± 0.2	124.5 ± 17.0	241 ± 19.7	0.5 ± 0.07
sUNC-13ΔLinker	3.2 ± 0.6	26.9 ± 2.0	41.0 ± 4.2	24.0 ± 2.6	40.6 ± 3.2	27.9 ± 1.4	41.9 ± 6.2	24.5 ± 3.0	3.2 ± 0.2	34.6 ± 5.4	303 ± 31.8	0.11 ± 0.02
sUNC-13ΔC2A	4.1 ± 1.2	23.6 ± 2.2	32.7 ± 3.8	19.5 ± 0.8	12.2 ± 1.1	21.4 ± 0.7	31.7 ± 2.2	21.6 ± 0.8	2.9 ± 0.2	59.7 ± 6.9	262 ± 46.6	0.23 ± 0.02
sUNC-13ΔLinker1	2.8 ± 0.4	24.7 ± 1.1	36.6 ± 3.5	24.7 ± 1.0	21.2 ± 2.1	27.0 ± 1.2	46.8 ± 3.9	26.2 ± 1.3	2.5 ± 0.2	23.0 ± 2.0	n/a	n/a
sUNC-13ΔLinker2	2.7 ± 1.0	24.6 ± 2.4	12.5 ± 2.9	20.7 ± 1.2	12.3 ± 1.4	30.5 ± 2.4	40.5 ± 4.0	28.4 ± 1.7	1.7 ± 0.14	12.7 ± 2.0	n/a	n/a
sUNC-13ΔLinker3	2.1 ± 0.5	23.8 ± 2.1	31.2 ± 2.3	24.4 ± 1.2	10.2 ± 0.9	28.2 ± 0.9	40.9 ± 3.1	25.9 ± 1.1	2.1 ± 0.3	18.0 ± 2.8	n/a	n/a
unc-64	0.9 ± 0.3	18.8 ± 2.3	6.4 ± 1.8	15.5 ± 1.3	2.2 ± 0.6	34.7 ± 2.4	38.5 ± 6.5	36.5 ± 2.3	0.14 ± 0.05	1.4 ± 0.03	113 ± 15.8	0.009 ± 0.003
UNC-64 rescue	1.6 ± 0.5	26.9 ± 2.2	35.2 ± 3.7	22.8 ± 1.8	10.5 ± 0.6	25.8 ± 1.4	46.3 ± 8.1	26.3 ± 2.4	1.5 ± 0.2	12.6 ± 1.6	211 ± 25.7	0.06 ± 0.007
sUNC-13;*unc-64*	0.6 ± 0.07	18.4 ± 1.7	5.7 ± 1.1	20.4 ± 1.5	0.7 ± 0.2	22.3 ± 4.5	23.0 ± 5.3	33.3 ± 2.5	0.15 ± 0.03	1.11 ± 0.03	n/a	n/a
UNC-64(open) rescue	11.9 ± 1.4	20.4 ± 1.0	48.9 ± 5.3	25.1 ± 1.6	35.3 ± 2.7	22.6 ± 0.9	54.4 ± 3.5	26.1 ± 1.7	2.5 ± 0.13	35.7 ± 2.8	251 ± 29.6	0.14 ± 0.03
sUNC-13;UNC-64(open)	14.9 ± 2.4	27.0 ± 1.6	46.8 ± 5.5	22.9 ± 1.7	27.5 ± 3.1	23.2 ± 1.3	41.4 ± 4.2	24.7 ± 1.6	3.2 ± 0.14	84.9 ± 14.1	285 ± 56.7	0.3 ± 0.05
cpx-1	33.8 ± 1.8	17.1 ± 0.9	95.4 ± 6.5	24.9 ± 1.3	31.9 ± 1.6	22.6 ± 1.0	52.7 ± 3.9	22.6 ± 0.7	0.23 ± 0.03	3.4 ± 0.6	n/a	n/a
cpx-1;unc-64	1.7 ± 0.3	21.0 ± 1.2	56.4 ± 1.9	22.0 ± 0.6	11.5 ± 1.1	24.3 ± 1.3	73.1 ± 6.4	30.3 ± 1.9	0.17 ± 0.02	3.2 ± 0.5	n/a	n/a
tom-1	1.8 ± 0.3	19.4 ± 1.3	45.8 ± 2.7	23.4 ± 1.0	11.0 ± 1.3	24.6 ± 0.9	42.9 ± 4.7	26.3 ± 2.3	3.8 ± 0.3	109.8 ± 18.7	310.1 ± 31.3	0.36 ± 0.06
tom-1;unc-64	0.65 ± 0.07	30.7 ± 3.9	7.3 ± 0.8	19.8 ± 2.2	0.98 ± 0.1	27.6 ± 4.0	15.3 ± 3.9	29.7 ± 3.1	0.78 ± 0.2	13.6 ± 4.5	n/a	n/a
sUNC-13;*tom-1*	23.8 ± 3.2	19.1 ± 0.7	n/a	n/a	32.2 ± 4.0	25.1 ± 1.6	n/a	n/a	3.1 ± 0.2	107.4 ± 15.9	n/a	n/a
UNC-64;*unc-13(s69)*	n/a	n/a	0.6 ± 0.09	20.9 ± 2.5	n/a	n/a	0.4 ± 0.04	23.2 ± 3.5	0.015 ± 0.01	0.055 ± 0.02	n/a	n/a
UNC-64(open);*unc-13(s69)*	n/a	n/a	1.3 ± 0.4	21.0 ± 1.9	n/a	n/a	2.9 ± 0.7	22.5 ± 1.3	0.06 ± 0.02	0.34 ± 0.13	n/a	n/a

All data were collected from 3 independent experiments to ensure the observed phenotypes were replicable. Data are presented as the mean +/- SEM.